

Numerical modeling of ocean currents and suspended sediment distribution in Benoa Bay, Bali

Siti Sulistiana*, I Wayan Nurjaya, and Mochamad Tri Hartanto

Department of Marine Science and Technology, Faculty of Fisheries and Marine Sciences, IPB University, 16680 Bogor, Indonesia

Abstract. Benoa Bay is a semi-enclosed water body that includes a shallow estuary area that supports important aquatic ecosystems, including mangrove ecosystems, seagrass beds, and coral reefs. The reclamation of Benoa Harbor and the construction of a toll road in Benoa Bay are suspected to have increased sedimentation. The objective of this study is to model ocean currents and suspended sediment distribution during the Northwest and Southeast monsoons in the waters of Benoa Bay. Numerical models are used to describe the hydrodynamic process as the main driver of the process of pollutant movement in the waters. The current pattern resulting from the model in the waters of Benoa Bay has the same pattern in the Northwest and Southeast Monsoons, with the current velocity of the Northwest Monsoon ranging from 0 – 1.6583 m/s and the Southeast Monsoon ranging from 0 – 1.4729 m/s. The distribution of suspended sediment in the Northwest Monsoon is quite high compared to the Southeast Monsoon. The distribution of suspended sediment in the Northwest Monsoon ranges from 0 – 846 mg/L and in the Southeast Monsoon, it ranges from 0 – 598 mg/L.

1 Introduction

Benoa Bay is a semi-enclosed water body located in the southeastern part of the island of Bali. Spanning the districts of Badung and the city of Denpasar, this water area includes shallow estuarine regions and features vital aquatic ecosystems, namely mangrove ecosystems, seagrass beds, and coral reefs. The attractiveness of this area has turned Benoa Bay into a hub for various human activities, including marine tourism, fish farming, a toll road, and a busy port with intensive shipping activities [1]. Reclamation activities on Serangan Island and the construction of the Bali Mandara Toll Road have resulted in uncontrolled sedimentation in this area due to the reduction of mangrove forests [2]. The Benoa Bay mangrove forest area is under tremendous pressure following the construction of the toll road and the conversion of mangrove land into ponds, settlements, and industrial areas [3]. Reclamation development in Benoa Port and the construction of a toll road across Benoa Bay are suspected to have increased sedimentation [4]. The distribution of suspended sediments in marine waters typically originates from the land and is transported to estuaries

* Corresponding author: sitisulistiana@apps.ipb.ac.id

by river discharge. This includes eroded material from upland areas, riverbed sediments, degradation by living organisms, and industrial and domestic wastes. Estuaries serve as points of exchange in the transport system, facilitating the flow of river runoff into ocean currents. Marine currents play a crucial role in sediment transport, as sediment is associated with both transport and deposition processes [5]. The waters of Benoa Bay are influenced by the discharge of six rivers (tukad) that flow into the bay. These rivers are Mati River, Badung River, Buaji River, Loloan River, Bualu River, and Sama River. The river mouths can result in direct input of organic waste into the bay, contributing to an increase in Total Suspended Solids (TSS). TSS refers to suspended particles in the water column, including soil particles (clay, silt, and sand), planktonic algae, and other materials ranging in size from 0.004 mm (clay) to 1.0 mm (sand). These materials play a role in causing sedimentation in the bay [6]. This study aims to describe the current patterns and distribution of suspended sediments in the Northwest and Southeast monsoons in the waters of Benoa Bay.

2 Method

2.1 Tools and materials

The data processing tools used for this research include a laptop computer with the specifications of an AMD Ryzen 3 3250U processor with Radeon graphics and 8 GB of RAM. In addition, the software used includes the numerical modeling tool OpenFlows FLOOD version 10.03.00.01, Ocean Data View, Microsoft Excel, QGIS version 3.28, Notepad, WRPLOT View (Wind Rose Plots for Meteorological Data), and Google Earth Engine. The research map is shown in Fig. 1.

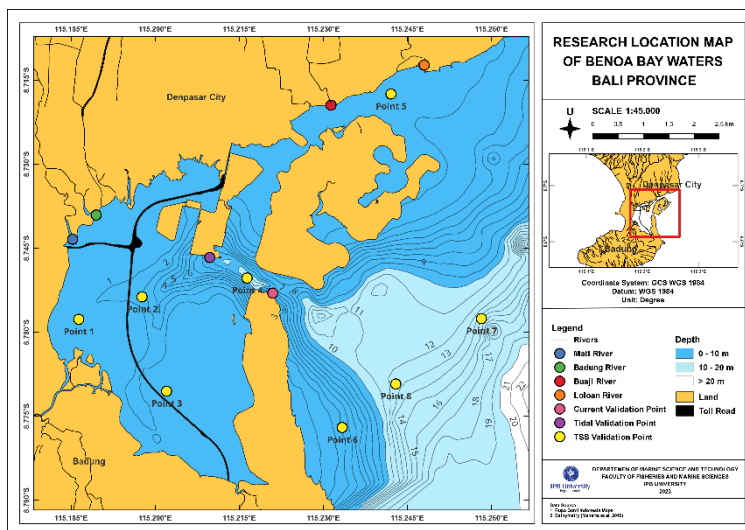


Fig. 1. Map of the research site in Benoa Bay waters.

The research data used to establish the model configuration include input data from various sources, including bathymetric data [1], FES2014 tidal data (www.avisio.altimetry.fr), ECMWF atmospheric components (<https://cds.climate.copernicus.eu/>), GloFAS river discharge data (<https://cds.climate.copernicus.eu/>), and Total Suspended Solids (TSS) concentration data [7, 8]. The validation data employed consisted of tidal data from Badan Informasi Geografis (BIG) (<https://srgi.big.go.id/>), current velocity data [1], Sentinel-2

satellite imagery data (<https://code.earthengine.google.com/>), and supporting data for the analysis of model results, such as precipitation data from Meteorology, Climatology, and Geophysical Agency (<https://dataonline.bmkg.go.id/>).

2.2 Research procedure

The research procedure in this study consists of three stages: pre-processing, processing, and post-processing of the model. The pre-processing stage involves configuring the model, including input data such as bathymetry, tidal components, atmospheric components, river discharge, and sediment distribution concentrations. The processing stage involves running the configured model, while the post-processing stage involves validating the model results and visualizing the model outputs, such as current patterns and suspended sediment distributions. Model configuration is performed for two seasons: the Northwest Monsoon (January 4 – 18, 2022) and the Southeast Monsoon (August 1 – 15, 2022).

2.3 Hydrodynamic and sediment transport equations

The hydrodynamic model uses the principles of the continuity equation from the Navier-Stokes equations with the Boussinesq approach (assuming constant water density) and hydrostatics [9]. The two-dimensional continuity equation is expressed as follows:

$$\frac{\partial u}{\partial x} + \frac{\partial v}{\partial y} = 0 \quad (1)$$

The hydrostatic pressure in the vertical momentum equation is expressed as follows:

$$\frac{\partial p}{\partial z} + \rho g = 0 \quad (2)$$

The momentum balance equations for horizontal velocities are in differential form and in cartesian coordinates using the following equations:

$$\frac{\partial u}{\partial t} + u \frac{\partial u}{\partial x} + v \frac{\partial u}{\partial y} - fv = -\frac{1}{\rho} \frac{\partial p}{\partial x} + \frac{\partial}{\partial x} \left(V_H \frac{\partial u}{\partial x} \right) + \frac{\partial}{\partial y} \left(V_H \frac{\partial u}{\partial y} \right) \quad (3)$$

$$\frac{\partial v}{\partial t} + u \frac{\partial v}{\partial x} + v \frac{\partial v}{\partial y} - fu = -\frac{1}{\rho} \frac{\partial p}{\partial y} + \frac{\partial}{\partial x} \left(V_H \frac{\partial v}{\partial x} \right) + \frac{\partial}{\partial y} \left(V_H \frac{\partial v}{\partial y} \right) \quad (4)$$

The TSS distribution model uses a concentration-based approach, as follows [10]:

$$\frac{\partial c}{\partial t} + u \frac{\partial c}{\partial x} + v \frac{\partial c}{\partial y} = \frac{\partial}{\partial x} \left(K_x \frac{\partial c}{\partial x} \right) + \frac{\partial}{\partial y} \left(K_y \frac{\partial c}{\partial y} \right) + (S_0 - S_i) \quad (5)$$

Where u and v are the components of the velocity vector in the x and y directions, f the Coriolis parameter, p is the pressure, V_H is the turbulent viscosities in the horizontal directions, K_x and K_y are Diffusion coefficient, S_0 is sediment input source, S_i is accretion or erosion sediment.

The deposition flux can be determined based on the following equation [11]:

$$S_d = \left(1 - \frac{\tau_b}{\tau_{cd}} \right) W_s C_b, \quad \tau_b \leq \tau_{cd} \quad (6)$$

The erosion flux can be determined based on the following equations [12]:

$$S_e = E \left(\frac{\tau_b}{\tau_{ce}} - 1 \right), \tau_b > \tau_{ce} \quad (7)$$

S_D is deposition rate, w_s is sediment fall velocity, C_b is subsurface concentration, τ_b is bed shear stress, τ_{cd} is critical bed shear stress for deposition, E is seabed erodibility, τ_{ce} is critical bed shear stress for erosion.

2.4 Model validation

Root Mean Square Error (RMSE) is an alternative method for evaluating forecasting techniques used to measure the accuracy of a model. The value produced by the RMSE is the average value of the square of the number of errors in the prediction model [13]. The RMSE is widely used to evaluate the relationship between the predicted and actual values of a model [14]. The smaller the RMSE value (closer to 0), the more accurate the prediction [15]. The RMSE calculation can be seen in the following formula:

$$RMSE = \sqrt{\frac{1}{n} \sum (y_t - y_{t+1})^2} \quad (8)$$

y_t is measurement data, y_{t+1} is model input data, n is total of measurement data. The calculation of the value of the correlation coefficient can be seen in the following formula:

$$r = \frac{S_{xy}}{S_x S_y}, -1 \leq r \leq 1 \quad (9)$$

S_{xy} is covariance between variables x and y , S_x is standard deviation of variable x , S_y is standard deviation of variable y . The correlation coefficient is a calculation that allows us to see the relationship or association between variables [16]. An r value close to 1 indicates a strong positive linear relationship.

2.5 Image data analysis

The algorithm used to determine the value of TSS (Total Suspended Solid) in the waters of Benoa Bay, namely the algorithm developed by Parwati [6]. The algorithm used is as in the following equation:

$$TSS(mg/L) = 3,3238 \times \exp(34,099 \times RedBand) \quad (10)$$

In this study, Sentinel-2 imagery was acquired directly from geospatial applications using Google Earth Engine, and image processing was performed based on this algorithmic calculation. The processed image data is visualized using the QGIS mapping application.

2.6 Scenario and model design

The model is run in two stages, namely the first stage by running a hydrodynamic model and the second stage by running a suspended sediment distribution model. The model is simulated in two different seasons, the Northwest Monsoon (January 4 – 18, 2022) and the Southeast Monsoon (August 1 – 15, 2022), to see the effect of different precipitation and river discharge on the model. The model domain is constructed using a constant-space grid with a grid size

of 33x33 m² and a time step of 4 seconds. There are two model boundaries, namely an open boundary in the form of waters located East of the bay and around the mouth of the river and a closed boundary in the form of land along the North, West, and South mainland edges of the study area. The input source of TSS is simulated from four estuaries, namely the Mati, Badung, Buaji, and Loloan rivers. The complete model configuration and design are shown in Table 1.

Table 1. Model configuration and design in Benoa Bay waters.

Parameter	Unit	Resolution
Number of cells X (I) grid	Cell	277
Number of cells Y (J) grid	Cell	280
Grid Size	m ²	33 x 33
Time Step	second	4
Domain Width	m	9141
Domain Length	m	9240
Depth	m	-
FES2014 Tides	m	1/16°
Atmospheric Pressure	Pa	1/4°
Solar Radiation	W/m ²	1/4°
Air Temperatures	°C	1/4°
Precipitation	mm	1/4°
Wind Speed	m/s	1/4°
Humidity	%	1/4°
Open Boundary Conditions	Degree (°)	115.2318 E 8.7909 S; 115.2620 E 8.7909 S; 115.2620 E 8.7078 S; 115.2618 E 8.7078 S; and the estuary area
Closed Boundary Conditions	-	Surrounding mainland and islands
Tidal Validation Points	Degree (°)	115.2098 E 8.7467 S
Current Validation Points	Degree (°)	115.2210 E 8.7529 S
Mati River Estuary Point	Degree (°)	115.1853 E 8.7436 S
Badung River Estuary Point	Degree (°)	115.1895 E 8.7391 S
Buaji River Muara Point	Degree (°)	115.2315 E 8.7196 S
Loloan River Estuary Point	Degree (°)	115.2480 E 8.7122 S
TSS Validation Points	Degree (°)	115.1864 E 8.7577 S; 115.1977 E 8.7537 S; 115.2021 E 8.7705 S; 115.2164 E 8.7503 S; 115.2421 E 8.7175 S; 115.2334 E 8.7770 S; 115.2583 E 8.7576 S; 115.2430 E 8.7692 S

3 Results and discussion

3.1 Model validation

The elevation of the tidal model compared to the BIG tidal data from January 4 – 18, 2022, is shown in Fig. 2. The root mean square error (RMSE) calculation yields a value of 0.0838 m, indicating that the hydrodynamic model results are close to the original values [17]. The correlation coefficient calculation also indicates a very strong relationship between the model results and the BIG data, with a value of 0.9891.

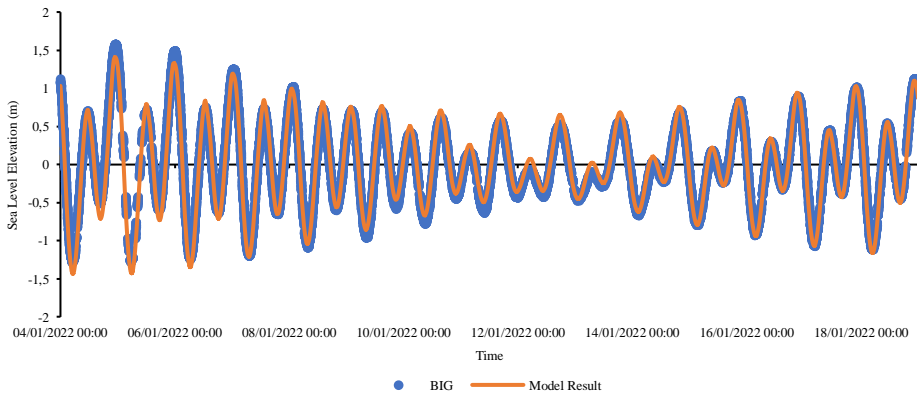


Fig. 2. The graph comparing BIG tidal data and the model results.

The validation of the currents was also conducted by comparing the hydrodynamic model current data with the measured current data [1] on June 25 – July 6, 2015 (Fig. 3). The RMSE values for the zonal current component (u) and the meridional current component (v) are 0.1544 m/s and 0.0888 m/s, respectively. These values are quite good, indicating that the model results have relatively small errors. In addition, the correlation coefficient calculations show a close relationship between the model results and the measured data. The correlation coefficient values for the zonal current component (u) are 0.8298, and for the meridional current component (v), it is 0.8435.

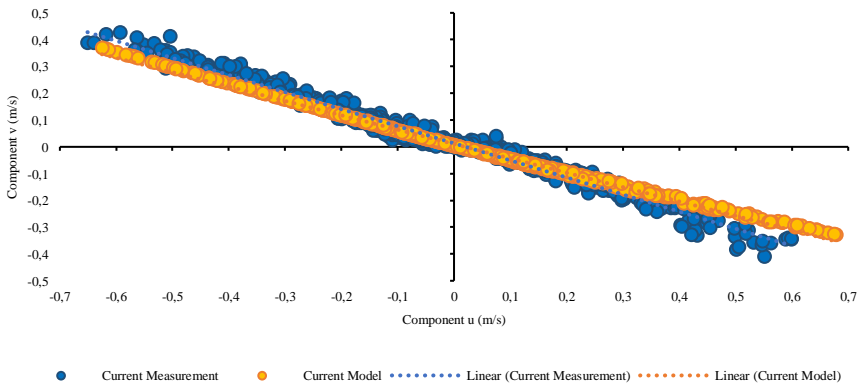


Fig. 3. The graph comparing measurement current velocity and model results.

3.2 The oceanographic conditions of Benoa Bay Waters

The oceanographic condition of Benoa Bay waters is seen from several parameters, namely depth, wind speed, tides, precipitation, and river water discharge. The depth of the water in Benoa Bay ranges from 0.5 to 22.3 meters, with depths inside the bay ranging from 0.5 to 10 meters and depths outside the bay ranging from 10 to 22.3 meters. This indicates that the waters of Benoa Bay fall into the category of shallow waters. The topographic features of Benoa Bay are shown on the survey map, Fig 1.

The wind speed during the Northwest monsoon ranges from 0.4180 to 8.9839 m/s, with an average of 4.0930 m/s. The wind speed during this season is mainly from the west. In the Southeast monsoon, the wind speed ranges from 0.5613 to 8.8840 m/s, with an average of 4.6620 m/s. The wind during this season is mainly from the Southeast. The wind movement significantly influences the dynamics of the surface current movement [18]. The wind direction and speed are visualized in Fig. 4.

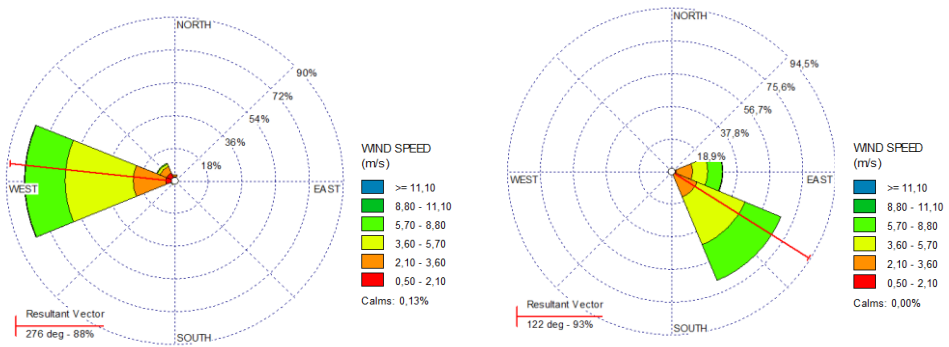


Fig. 4. Wind direction (left) Northwest Monsoon and (right) Southeast Monsoon of Benoa Bay.

The tidal range (Fig. 2) indicates that the waters of Benoa Bay have a mixed, mainly semidiurnal pattern, with a Formzahl value of 0.3625. This means that there are two high tides and two low tides per day, but occasionally there is one high tide and one low tide. Tidal fluctuations in this area have the Highest High Water Level (HHWL) of 1.5769 meters and the Lowest Low Water Level (LLWL) of 1.2831 meters. The tidal components used to calculate the form number are analyzed using the Admiralty method.

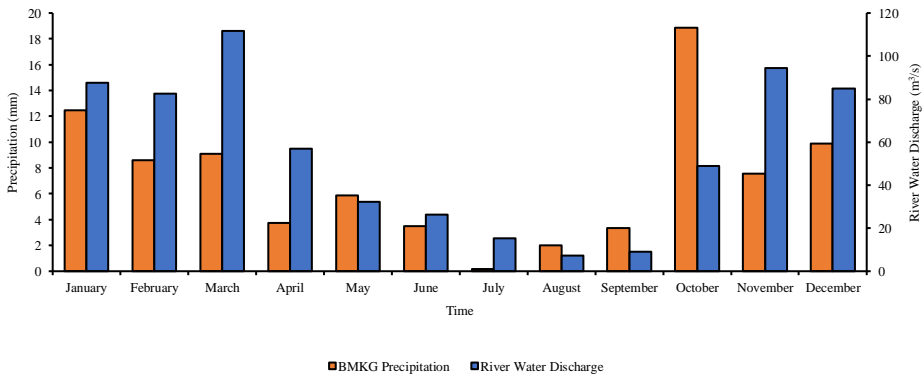


Fig. 5. The graph of average monthly precipitation and river discharge at Benoa Bay.

The precipitation during the Northwest Monsoon (December, January, and February) tends to be higher compared to the Southeast Monsoon (June, July, and August). The average precipitation during the Northwest Monsoon is 10 mm, while during the Southeast Monsoon, it is 2 mm. The value of precipitation tends to increase in the Northwest Monsoon due to the Asian monsoon, which carries a high mass of water vapor [19]. These precipitation values are reflected in the river discharge, as an increase in precipitation corresponds to an increase in river discharge. The average river discharge during the Northwest Monsoon is 85 m³/s, and during the Southeast Monsoon, it is 16 m³/s. Precipitation and river discharge in the waters of Benoa Bay are shown in Fig. 5.

3.3 The ocean current and suspended sediment distribution models

Ocean current is one of the oceanographic parameters that plays a critical role in determining the conditions of a water body. The patterns and characteristics of currents, such as the dominant type, speed, and direction, as well as the pattern of ocean current movement, make the conditions of a water body dynamic [20]. Currents represent the movement of water masses influenced by internal and external forces. Internal forces that influence ocean currents include factors such as differences in seawater density, shallow pressure gradients, and upwelling. External forces affecting ocean currents include wind, gravitational forces, the gravitational pull of the sun and moon on the Earth, tectonic forces, and the Coriolis force [4]. Current simulations were conducted during two seasons, the Northwest Monsoon and the Southeast Monsoon, as shown in Fig. 6 and 7.

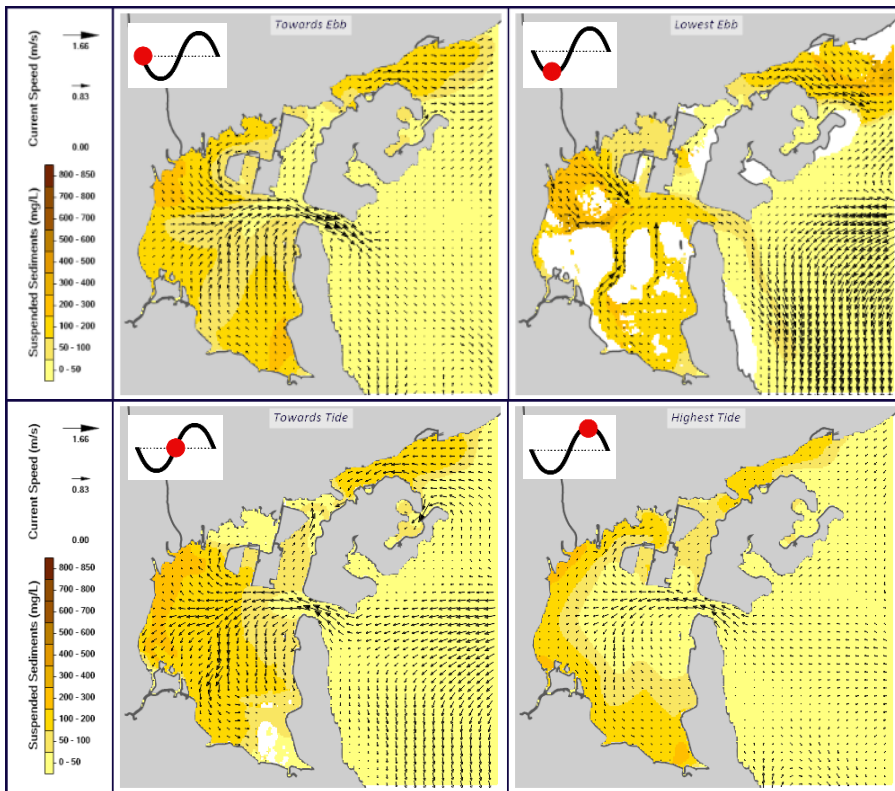


Fig. 6. Ocean currents and suspended sediment distribution in Benoa Bay during the Northwest Monsoon.

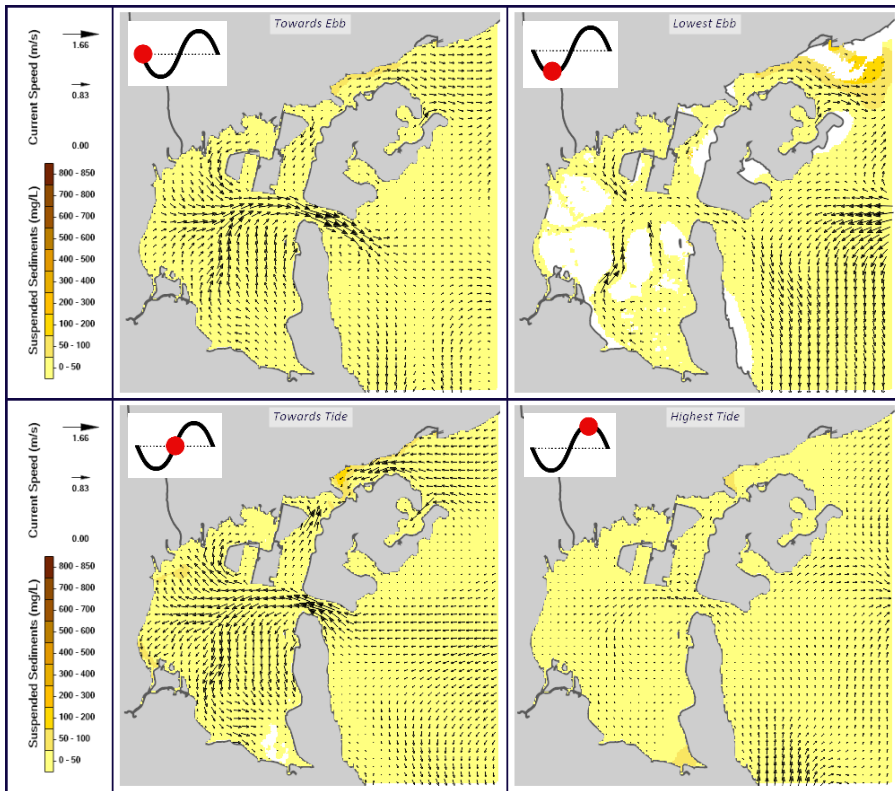


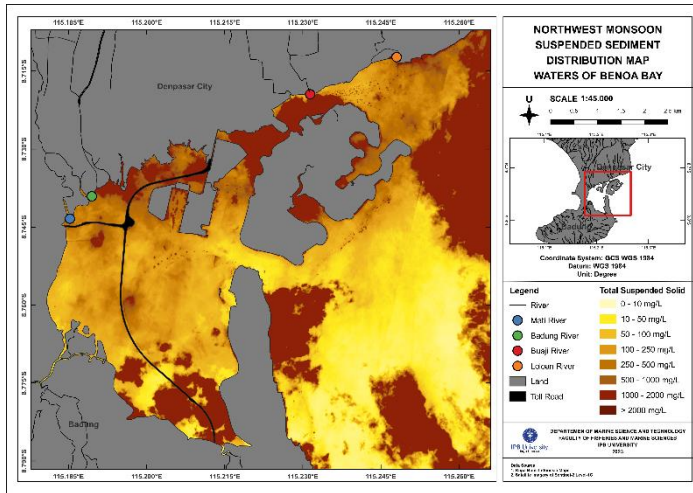
Fig. 7. Ocean currents and suspended sediment distribution in Benoa Bay during the Southeast Monsoon.

The current speed during the northwest monsoon ranges from 0 to 1.6583 m/s, while during the southeast monsoon it ranges from 0 to 1.4729 m/s. The current pattern in each season has the same pattern, the current flows out of the bay during low tide, and the current reverses direction and flows into the bay during high tide. This indicates that the currents in the waters of Benoa Bay are influenced by tidal movements. Tidal forces are a major driving factor in the mass circulation of water in narrow and semi-enclosed water bodies, such as straits and bays [21].

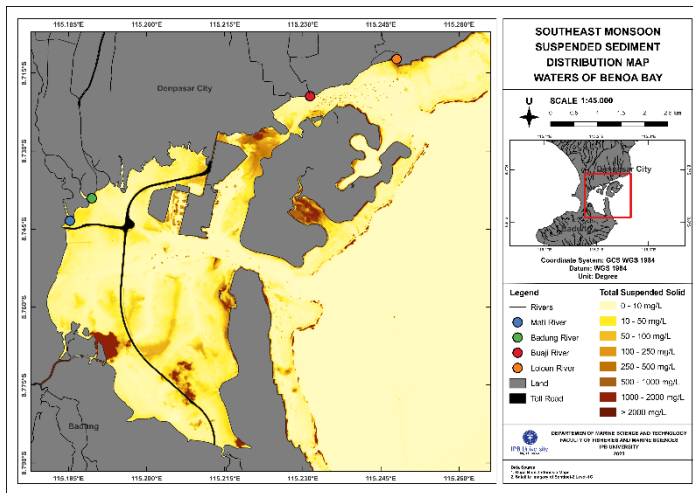
Suspended sediment refers to both organic and inorganic materials that float in the water column before settling to the bottom of the water body. Suspended sediments can cause pollution that leads to turbidity in the water [5]. This suspended sediment can be in the form of silt, clay, fine sand, specific organic matter, microbial cells, and microscopic organisms transported into the water by soil erosion [22]. Simulations of sediment distribution were also conducted during two seasons, namely the Northwest Monsoon and the Southeast Monsoon, as shown in Fig. 6 and 7. The distribution of suspended sediment during the northwest monsoon ranges from 0 to 846 mg/L, while during the southeast monsoon it ranges from 0 to 598 mg/L. There are four simulated sources of suspended sediment inputs to the waters of Benoa Bay, namely inputs from the estuaries of Mati River, Badung River, Buaji River, and Loloan River. Inputs from the estuaries of the Mati River and Badung River contribute to the movement of the current pattern towards the mouth of the bay, extending towards the southern part of the bay. Meanwhile, inputs from the estuaries of the Buaji River and Loloan River flow directly into the open waters outside the bay.

3.4 Suspended sediment distribution from satellite imagery

The images used in the research are Sentinel-2 images acquired during the Northwest Monsoon, specifically from January 4 to 18, 2022, and the Southeast Monsoon, from August 1 to 15, 2022. Sentinel-2 imagery will be used to map the distribution patterns of Total Suspended Solids (TSS) in the waters of Benoa Bay and serve as validation data for the suspended sediment distribution model. The suspended sediment distribution based on the Northwest Monsoon and Southeast Monsoon imagery is shown in Fig. 8a and 8b.



(a)



(b)

Fig. 8. Suspended sediment distribution during the (a) Northwest Monsoon (b) Southeast Monsoon.

The map of suspended sediment distribution during the Northwest Monsoon and Southeast Monsoon shows differences in total suspended solids (TSS) concentrations. Suspended sediment distribution during the Northwest Monsoon appears higher compared to the Southeast Monsoon. The TSS values during the Northwest Monsoon around the estuaries are as follows: Mati River estuary 202 mg/L, Badung River estuary 482 mg/L, Buaji River estuary 201 mg/L, and Loloan River estuary 336 mg/L. During the southeast monsoon, the

TSS values around the estuaries are as follows: Mati River estuary 38 mg/L, Badung River estuary 20 mg/L, Buaji River estuary 33 mg/L, and Loloan River estuary 34 mg/L.

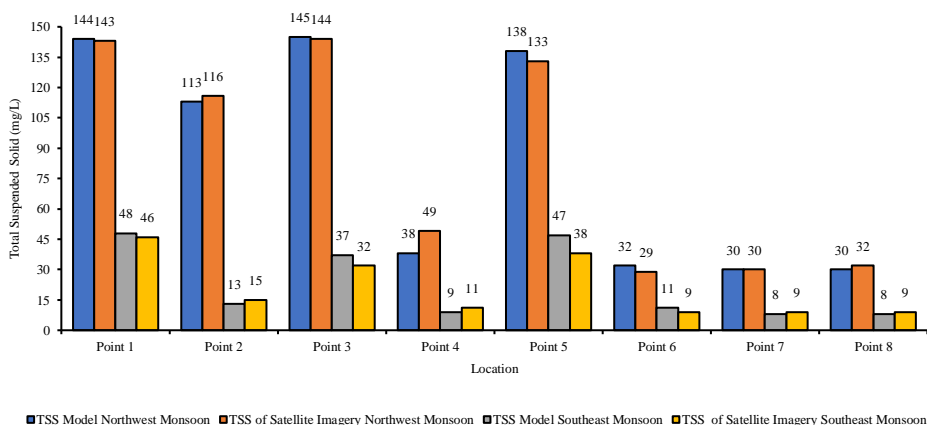


Fig. 9. The graph compares the Total Suspended Solids values of the model and image results.

The graph comparing the Total Suspended Solids (TSS) values from the model and the images (Fig. 9) at the same 8 points is used to assess the accuracy of the model data against the image data. The graph shows that the TSS values from the model are relatively close to the TSS values from the images, as the generated values are not significantly different during both the Northwest Monsoon and the Southeast Monsoon. In addition, the TSS values appear to be higher during the Northwest Monsoon compared to the Southeast Monsoon. This is attributed to the river flow into Benoa Bay with a higher water intensity during the Northwest Monsoon compared to the Southeast Monsoon, indicating that seasonal factors can determine the TSS distribution in the waters, influenced by both tidal factors and differences in precipitation intensity.

4 Conclusion

The ocean current of the model results in the waters of Benoa Bay Bali has the same pattern in the Northwest Monsoon and the Southeast Monsoon, which is that the current will move towards the outside of the bay at low tide and the current will reverse direction and enter towards the inside of the bay at high tide. The current speed of the Northwest Monsoon ranges from 0 – 1.6583 m/s and that of the Southeast Monsoon ranges from 0 – 1.4729 m/s. The suspended sediment distribution in the Northwest Monsoon is higher than that in the Southeast Monsoon. This is influenced by the high precipitation factor in the Northwest Monsoon and has an impact on the input of TSS concentrations into the waters. The distribution of suspended sediment in the Northwest Monsoon ranges from 0 – 846 mg/L and in the Southeast Monsoon, it ranges from 0 – 598 mg/L. Weak currents around the estuary cause faster TSS deposition.

References

1. I.P.R.F. Maharta, I.G. Hendrawan, Y. Suteja, *Journal of Marine and Aquatic Sciences*, **5**(1):44–54 (2019)

2. I.K.A.S. Putra, N. Bashit, Y. Wahyuddin, *Jurnal Geodesi Undip*, **10**(2):58–68 (2021)
3. D.B. Wiyanto, E. Faiqoh, *Journal of Marine and Aquatic Sciences*, **1**(1):1–7 (2015)
4. T.A. Tanto, A. Putra, G. Kusumah, A.R. Farhan, W.S. Pranowo, S. Husrin, Ilham, *Jurnal Kelautan Nasional*, **12**(3):101–107 (2017)
5. S.E. Arvianto, A. Satriadi, G. Handoyo, *Jurnal Oseanografi*, **5**(1):116–125 (2016)
6. G.Y. Kamajaya, I.D.N.N. Putra, I.N.G. Putra, *Journal of Marine and Aquatic Sciences*, **7**(1):18–24 (2021)
7. I.G.S. Risuana, I.G. Hendrawan, Y. Suteja, *Journal of Marine and Aquatic Sciences*, **3**(2):223–232 (2017)
8. N.M. Ernawati, I.W. Restu, *Jurnal Enggano*, **6**(1):25–36 (2021)
9. H. de Pablo, J. Sobrinho, M. Garcia, F. Campuzano, M. Juliano, R. Neves, *Water*, **11**(1713): 1–23 (2019)
10. I.W. Nurjaya, H. Surbakati, N.M.N. Natih, *IOP Conf. Series: Earth and Environmental Science*, **278** 012056 (2019)
11. R.B. Krone, *Flume Studies of The Transport of Sediment in Estuarial Shoaling Processes* (University of California, Berkeley, 1962)
12. A.J. Mehta, E.J. Hayter, R.W. Parker, R.B. Krone, A.M. Teeter, *Journal of Hydraulic Engineering*, **115**(8):1076–1112 (1989)
13. V.R. Prasetyo, H. Lazuardi, A.A. Mulyono, C. Lauw, *Jurnal Nasional Teknologi dan Sistem Informasi*, **7**(1):8–17 (2021)
14. W. Wang, Y. Lu, *IOP Conference Series: Materials Science and Engineering*, **324**(1):1–10 (2018)
15. R.Y. Hayuningtyas, R. Sari, *Jurnal Teknik Komputer AMIK BSI*, **8**(1):40–44 (2022)
16. HY. Kim, *Restor Dent Endod*, **43**(1):1–7 (2018)
17. H.W. Herwanto, T. Widiyaningtyas, P. Indriana, *Jurnal Nasional Teknik Elektro dan Teknologi Informasi*, **8**(4): 364–370 (2019)
18. U. Fadika, A. Rifai, B. Rochaddi, *Jurnal Oseanografi*, **3**(3):429–437 (2014)
19. R. Hidayat, K. Ando, *J Agromet Indonesia*, **28**(1):1–8 (2014)
20. L.C. Permadi, E. Indrayanti, B. Rochaddi, *Jurnal Oseanografi*, **4**(2):516–523 (2015)
21. Y.S.A. Wibowo, Hariadi, J. Marwoto, *Jurnal Oseanografi*, **5**(4): 490–497 (2016)
22. N.L. Ma'arif, Z. Hidayah, *Juvenil*, **1**(3): 417–426 (2020)